

# Synthesis and characterization of nanostructured Bi<sub>2</sub>O<sub>3</sub>-doped cerium oxides fabricated by PVA polymerization process

Zhi-Cheng Li <sup>a,\*</sup>, Hong Zhang <sup>a</sup>, Bill Bergman <sup>b</sup>

<sup>a</sup> School of Materials Science and Engineering, Central South University, Hunan Changsha 410083, PR China

<sup>b</sup> Department of Materials Science and Engineering, School of Industrial Engineering and Management, Royal Institute of Technology, SE 10044 Stockholm, Sweden

Received 30 April 2007; received in revised form 1 May 2007; accepted 6 July 2007

Available online 17 August 2007

## Abstract

Bi<sub>2</sub>O<sub>3</sub>-doped ceria oxygen-ion conductors were prepared by a wet chemical synthesis method, which is performed by polymerization of polyvinyl-alcohol (PVA). The experiments showed that Bi<sub>2</sub>O<sub>3</sub>–CeO<sub>2</sub> solid solution with 9.2 nm grains and pure fluorite type phase can be synthesized at a calcination temperature of 500 °C by PVA polymerization process. X-ray analysis revealed that high density nanostructured bulks could be prepared at a sintering temperature of 900 °C, and these bulk samples with an average grain size less than 70 nm could effectively be obtained at various heating rates during sintering. Oxygen-ion conductivity increased with the increase of dopant concentrations between 5 mol% and 15 mol% in present study.

© 2007 Elsevier Ltd and Techna Group S.r.l. All rights reserved.

**Keywords:** Ceria-based conductor; Bi<sub>2</sub>O<sub>3</sub> dopant; Synthesis; PVA polymerization process; Conductivity

## 1. Introduction

Oxygen ionic conductors have been used in various applications, such as oxygen sensors, oxygen pumps, and solid oxide fuel cells (SOFCs) [1–3]. In these applications, SOFCs have attracted much attention because they offer various potential advantages, such as a wide variety of available fuels, a good durability, inexpensive technology and a potential advantage of high efficiency. A typical SOFC has an electrolyte with 8 mol% yttria-stabilized zirconia (YSZ). YSZ-based SOFC is required to operate at high temperature of 800–1000 °C. However, at high operating temperatures, some harsh factors such as the sealing problem, thermal mismatch between materials, and interfacial reactions at electrode/electrolyte interfaces and electrode/interconnector interfaces, may occur, decreasing the efficiency and stability of the cell, leading to high manufacturing and maintenance costs and application limitation for SOFCs [4].

In order to reduce the operating temperature, some novel oxygen-ion conductors including CeO<sub>2</sub>-, Bi<sub>2</sub>O<sub>3</sub>- and

LaGaO<sub>3</sub>-based oxides have been extensively investigated [5–7]. These materials have a much higher ionic conductivity at relatively lower temperatures in comparison to that of YSZ. Doped cerium oxides have extensively been studied as one of the most promising candidates for application as solid electrolyte for intermediate temperature SOFCs. Di- or trivalent metal oxides such as calcia (CaO) or rare-earth oxide are always selected as dopants for CeO<sub>2</sub> oxide. Among various doped cerium oxides, Sm<sub>2</sub>O<sub>3</sub>-doped ceria was reported to have the highest conductivity, and has obtained a lot of attention [8–12].

Many different powder synthesis techniques have been used for preparation of ceria-base electrolytes. However, sintering temperatures were always high, e.g. the sintering temperature is higher than 1550 °C for Sm-doped ceria in a conventional solid state reaction process [11], and temperatures higher than 1500 °C for Gd<sup>3+</sup>/Sm<sup>3+</sup> co-doped cerium oxides in co-precipitation or hydrothermal method [12]. Reports about Bi<sub>2</sub>O<sub>3</sub>–CeO<sub>2</sub> oxides showed that the possibility of obtaining a pure single phase solid solution was depending on the synthesis route, e.g. Chen and Eysel [13] failed to prepare solid solutions (CeO<sub>2</sub>)<sub>1±x</sub>(BiO<sub>1.5</sub>)<sub>x</sub> by the high temperature ceramic method. Hydrothermal synthesis seems to be a good route for

\* Corresponding author. Tel.: +86 731 8877 740; fax: +86 731 8876 692.

E-mail address: [zhchli@mail.csu.edu.cn](mailto:zhchli@mail.csu.edu.cn) (Z.C. Li).

preparation of nanostructural Bi-doped  $\text{CeO}_2$  [14], but it is limited for the industrial application because of its harsh synthesis conditions and high cost, such as, high temperature, high pressure and long reaction time in the autoclave. Therefore, it is of interest to study the synthesis of these solid solutions by low temperature reaction routes. In this paper, we report a so-called steric entrapment synthesis (SES) process by polymerization of polyvinyl-alcohol (PVA) for preparation of nanostructured  $\text{Bi}_2\text{O}_3$ -doped ceria oxides. Pure fluorite-type phase with average grain size of 9.2 nm was fabricated at a calcination temperature of 500 °C, and high density nanostructured bulk samples with high conductivity could be obtained at a sintering temperature of 900 °C.

## 2. Experimental procedures

$\text{Ce}_{1-x}\text{Bi}_x\text{O}_2$  ( $x = 0.05, 0.07, 0.10, 0.12$  and  $0.15$ ) solid solutions were prepared by a wet chemical method, the so-called steric entrapment synthesis (SES) process, involving polymerization of polyvinyl-alcohol (PVA). The raw materials were  $\text{CeO}_2$  (>99.5%, Merck KGaA, Germany),  $\text{Bi}_2\text{O}_3$  (>99.5%, Merck KGaA, Germany) and Polyvinyl alcohol (PVA, 98–99%, Alfa Aesar, a Johnson Matthey Company, Germany). Raw materials were weighed according to calculated amount for each experimental batch.  $\text{CeO}_2$  was dissolved into  $\text{HNO}_3$ – $\text{H}_2\text{O}_2$  mixed aqueous solution,  $\text{Bi}_2\text{O}_3$  was dissolved into  $\text{HNO}_3$  aqueous solution, and PVA was dissolved into distilled water, respectively. Then the dissolved salt solutions and PVA solution were mixed at a ratio of one mole PVA to 1 mol cations, resulting in the precursor solution. This mixed solution was heated at about 150 °C while stirring until the water had evaporated. As a result, a crisp gel was obtained, and was ground into powder. Calcination was performed in air in a tube furnace at temperatures between 500 °C and 800 °C for 1 h. The heating rate was 5 °C/min.

About 700 °C calcined powder was granulated with PVA solution, and pressed into pellets with diameter of 15 mm and thickness of 2.5 mm. The pressure was 200 MPa. Sintering was performed at 900 °C for 1 h in air. During sintering, heating rates were selected at 5 °C/min, 10 °C/min and 16 °C/min, respectively, followed by furnace cooling. Where, the heating rates of 5 °C/min and 10 °C/min were controlled by programs in a box furnace (model VMK 1800, Linn High Therm GmbH, Germany). The sintering at 16 °C/min heating rate was made in a tube furnace and the heating rate was calculated by dividing the selected sintering temperature, 900 °C, by temperature-increasing time, 50 min. That means the 16 °C/min heating rate was an average rate.

Calcined powders and sintered samples were analyzed by X-ray powder diffraction (XRD) (HUBER Imaging Plate Guinier Camera G670, with  $\text{Cu K}\alpha$  radiation) operating at room temperature. The sintered pellets were ground to a thickness of about 1 mm and painted with gold paste on both parallel sides of the samples as the electrode. AC conductivities were characterized by an EI300 electrochemical impedance spectroscopy (Gamry Instruments, Inc.). The range of AC frequency is 0.01 Hz to 300 KHz.

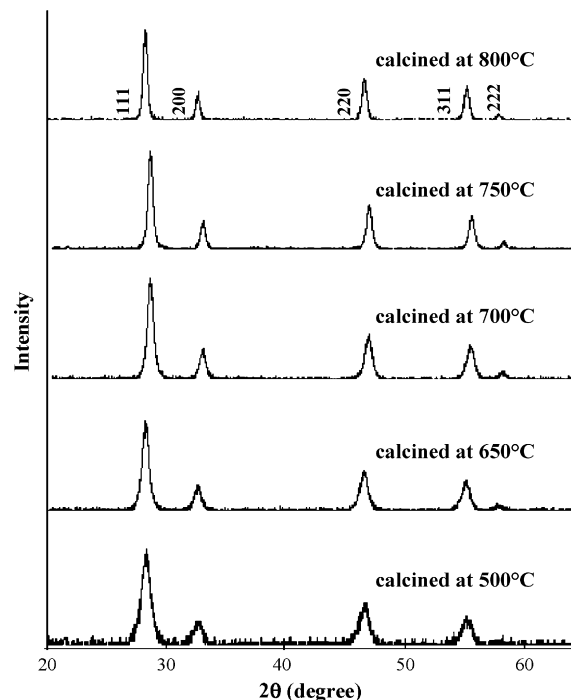


Fig. 1. XRD patterns of  $\text{Bi}_2\text{O}_3$ -doped  $\text{CeO}_2$  powders calcined at different temperatures.

## 3. Results and analysis

### 3.1. Phase and microstructure

Fig. 1 shows the XRD spectra of the  $\text{CeO}_2$  based oxide powders doped with  $\text{Bi}_2\text{O}_3$  concentration of 10 mole% and calcined at 500, 650, 700, 750 and 800 °C, respectively. Strong XRD Bragg peaks indicated a fluorite type phase, to which  $\text{CeO}_2$  belongs. Bragg peaks of monoclinic  $\alpha$ - $\text{Bi}_2\text{O}_3$  phase or cubic  $\beta$ - $\text{Bi}_2\text{O}_3$  phase were not found in any of the obtained XRD spectra. This reveals that a pure fluorite-type phase had been obtained after all calcinations.

At the same time, broadened XRD Bragg peaks indicated fine-grain powders. In order to analyze the grain size, (1 1 1) Bragg peaks were separated from all XRD spectra and are shown in Fig. 2. The half-width height of the Bragg peaks decreased with increasing calcination temperature. Average grain size calculated by Debye–Scherrer method for each powder is listed in Table 1. 10 mole%  $\text{Bi}_2\text{O}_3$ -doped  $\text{CeO}_2$

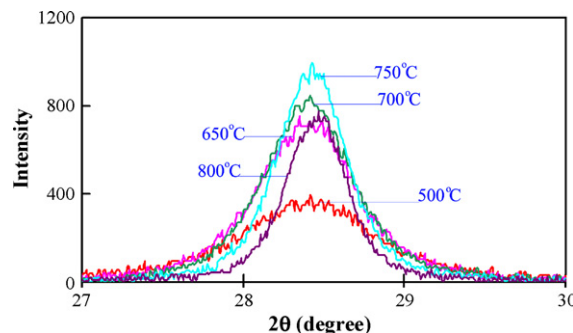


Fig. 2. (1 1 1) XRD peaks of the doped ceria calcined at various temperatures.

Table 1

Calculated grain size of Bi<sub>2</sub>O<sub>3</sub>-doped ceria powders calcined at different temperatures

Calcination temperatures (°C)	Grain size (nm)
500	9.2
650	11.9
700	12.7
750	15.2
800	16.9

powders with the grain sizes from 9.2 nm to 16.9 nm had been obtained after calcinations by SES process.

The above XRD analysis revealed that the grain size of nanostructured Bi<sub>2</sub>O<sub>3</sub>-doped CeO<sub>2</sub> slightly increased with increasing calcination temperature, and pure phase could be easily obtained. It is generally accepted that synthesis of ceramics by wet-chemical method is preferred to those employing reaction in the solid state, because it gives rise to more homogeneous powders with controlled composition. The steric entrapment synthesis method, a polymerized organic-inorganic route, that uses simple, long-chain polymers such as PVA as the carrier phase is a viable, simple, inexpensive technique for producing mixed-oxide powders, in comparison with other wet-chemical methods such as the Pechini method [15,16]. These simple polymer chains have no special chelating end groups, in contrast to the  $\alpha$ -pyroxy-carboxylic acid of the Pechini precursor. In aqueous PVA solutions, metal ions can be stabilized by the polymer via interaction with the hydroxyl groups. Even if some cations do not have a direct link to the hydroxyl groups, they are localized around the polymer by the bridging action of the water molecules between the metal ions that are linked to the hydroxyl groups and the free-floating metal ions. During precursor processing, the water of solution evaporates, the free space between the polymer molecules shrinks and the chain entanglement causes a close polymer. The cation mobility is greatly reduced and the water remaining in the precursor keeps all the cations in the entanglement polymer network. As a result, no precipitation causes off-stoichiometry, and homogeneous powder can be obtained.

Fig. 3 shows XRD spectra of the 10 mole% Bi<sub>2</sub>O<sub>3</sub> doped ceria calcined at 700 °C for 1 h and sintered at 900 °C for 1 h with heating rates of 5 °C/min, 10 °C/min and 16 °C/min, respectively. After the sintering, all bulk samples have a pure fluorite

CeO<sub>2</sub> structure, and there was not any XRD Bragg peak from secondary phases. Grain sizes of the sintered samples were also calculated by the Debye–Scherrer method. The average size is 69 nm, 35.9 nm and 29 nm respectively for the heating rates of 5 °C/min, 10 °C/min and 16 °C/min, respectively. The bulk samples showed only slight grain growth compared with calcined powder. It should be noted that there was not much difference between the grain sizes at the heating rates of 10 °C/min and 16 °C/min. But microcracks were found inside the samples heated at 16 °C/min. Those microcracks, thermal cracks, might result from the quick heating and inhomogeneous shrinking for the larger heating rate during sintering.

The relative density of the sintered bulks was determined by dividing the bulk density of the samples by the theoretical density. The theoretical density, 4.319 g/cm<sup>3</sup>, was calculated by using the lattice parameter  $a = 0.5422$  nm obtained from the XRD analysis. The relative density of pellets sintered at 900 °C at various heating rates was between 96.8% and 98%. Lattice parameter was analyzed according to Bragg formula from the XRD spectra as showed in Fig. 3. The cell parameter of the doped solid solution is  $a = 0.5422$  nm, while the one of pure CeO<sub>2</sub> crystal is 0.5412 nm [14]. The slightly enlarged cell parameter was ascribed to the larger lattice distortion due to the dopant Bi<sup>3+</sup>, because the ionic radius of Bi<sup>3+</sup> ion is larger than the one of Ce<sup>4+</sup> ion. For a coordination number of 8 in fluorite crystal, Bi<sup>3+</sup> and Ce<sup>4+</sup> ions have ionic radii 0.131 nm and 0.1283 nm, respectively [17].

### 3.2. Conductivity measurements

The conductivity of the samples was measured by an AC complex impedance method, and the applied frequency range of AC is from 0.01 Hz to 300 KHz. Generally, an impedance spectrum for an ionic conductor consists of three parts, a bulk (grain) semicircle, a grain-boundary semicircle and an electrode-process arc.

Fig. 4a shows the Nyquist-plotted impedance spectra of the ceria samples, doped by various Bi<sub>2</sub>O<sub>3</sub> concentrations, measured at 300 °C. The real part of impedance decreased with increasing dopant content. No grain boundary semicircle could be detected in the spectra. This should result from the pure single phase and nanometer crystalline structure. Because secondary phases and impurities located at grain boundaries always are poor ionic conductors, resulting in impedance increase at grain boundaries. Fig. 4b shows the temperature dependence of the conductivity. All these samples were sintered at 900 °C at a heating rate of 5 °C/min. The conductivity increased with increasing dopant concentration. At temperatures below 500 °C, the  $\ln(\sigma T)$  varies linearly with  $1/T$ . However, when the temperature was higher than 500 °C, this linear relationship changed, and all related activation energies, as listed in Table 2, decreased. Similar phenomena exist in LaGaO<sub>3</sub>-based oxides [15,18], and can be explained as the following. The dopant ions acted not only as traps for isolated oxygen vacancies, but also as nucleating sites for the formation of ordered-vacancy clusters. At lower temperatures, the oxygen vacancies were progressively trapped into the clusters; at higher temperatures, the vacancies could be

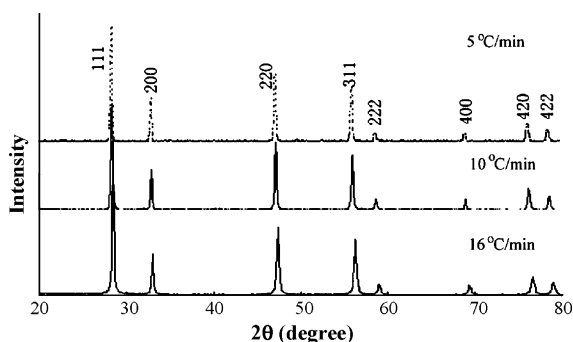


Fig. 3. XRD pattern of Bi<sub>2</sub>O<sub>3</sub>-doped CeO<sub>2</sub> sample sintered at 900 °C at heating rates of 5 °C/min, 10 °C/min and 16 °C/min, respectively.

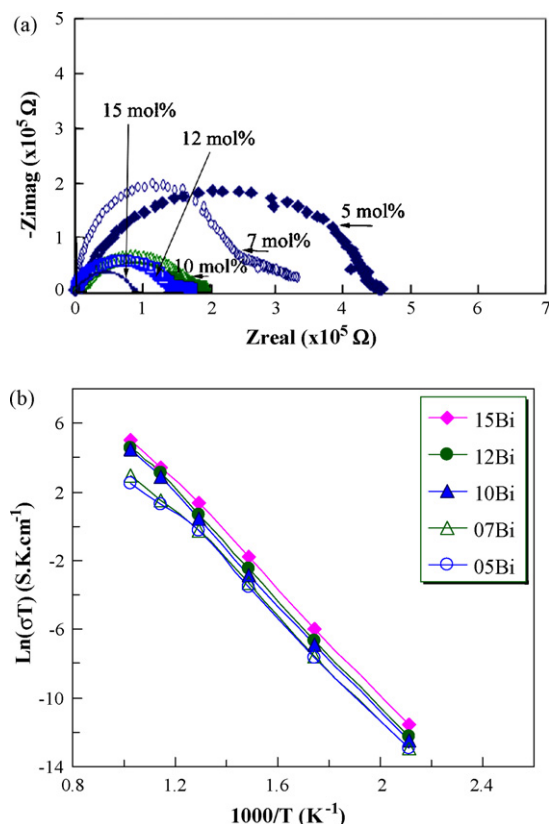


Fig. 4. Conductivity of ceria oxides doped with various  $\text{Bi}_2\text{O}_3$  concentrations, (a) Impedance spectra in Nyquist plot recorded at 300 °C, and (b) Arrhenius plots.

dissolved into the matrix of the oxygen sites. The porosities could also catch the oxygen ions and affect the conductivity. In this case, the pores were trapped in the grains or grain boundaries, blocking oxygen ion migration, resulting in the lower conductivity.

In Fig. 5a the Nyquist-plotted impedance spectra of 10 mol%- $\text{Bi}_2\text{O}_3$ -doped samples measured at 300 °C is shown. Those samples were calcined at 700 °C and then sintered at 900 °C at heating rates of 5 °C/min, 10 °C/min and 16 °C/min, respectively. There was no grain-boundary arc in any spectrum. Fig. 5b shows the Arrhenius plots of the conductivity for 10 mol%  $\text{Bi}_2\text{O}_3$ -doped ceria samples depending on heating rates during sintering. The sample sintered at the heating rate of 10 °C/min had the highest conductivities at all measured temperatures. At 400 °C, the conductivities is  $3.98 \times 10^{-4}$  S/cm, similar to the reported Bi-doped  $\text{CeO}_2$  [14]. When the

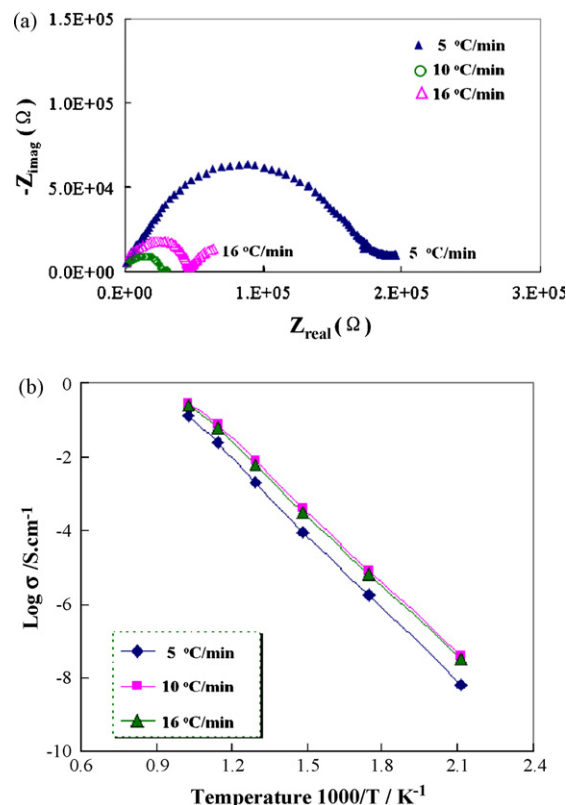


Fig. 5. Conductivity of  $\text{Bi}_2\text{O}_3$ -doped ceria samples at various heating rates during sintering, (a) Impedance spectra at 300 °C, and (b) Conductivities in Arrhenius plots.

operating temperatures are higher than 500 °C, the conductivities are higher than those in Sm- and Gd- doped  $\text{CeO}_2$  oxides [19,20]. The sample sintered at heating rate of 16 °C/min had finer grains than the other two groups of samples, but it showed slightly lower conductivity than that of the sample sintered at the heating rate of 10 °C/min. The reason should be that microcracks, which affected the ionic transport, had formed inside the sample sintered at the heating rate of 16 °C/min.

Materials with nanostructures could show novel effects on the conductivity. A nanostructured bulk sample has a large grain-boundary area, which consists of a large amount of defects, assisting the transference of oxygen ions, comparing with those conductors with the grain size in micrometer scale. This is in agreement with the previous reports in Refs. [21–23], in the case of nanostructured solid electrolytes, that grain-boundary diffusion played an important role because the volume fraction of grain boundaries is much larger, and the diffusion is much faster than bulk diffusion. In present experiments, nanostructured materials, including both powder and bulk samples, were obtained, and the fabricated oxides showed high conductivities. These indicated that PVA polymerized synthesis method was an effective route for the preparation of nanocrystalline materials.

#### 4. Conclusions

The PVA polymerization wet-chemical synthesis method is an effective process for the preparation of  $\text{Bi}_2\text{O}_3$ -doped ceria

Table 2  
Activation energies of the  $\text{Bi}_2\text{O}_3$ -doped ceria for different dopant contents

Dopant concentration (mol%)	Activation energy (eV) at 200–500 °C	Activation energy (eV) at 500–700 °C
5	1.335	0.897
7	1.335	1.046
10	1.356	1.303
12	1.356	1.270
15	1.359	1.196

fast ionic conductor. Nanostructured powders with a pure fluorite-type  $\text{Bi}_2\text{O}_3\text{--CeO}_2$  solid solution were fabricated at the calcination temperatures from 500 °C to 800 °C, and the average grain sizes were from 9.2 nm to 16.9 nm, respectively. Nanocrystalline bulks with single phase and high density were obtained when the samples were sintered at 900 °C. The conductivity increased with the increase of dopant concentrations. The samples sintered at 900 °C and heating rate of 10 °C/min had the average grain size of 35.9 nm, and showed higher conductivity than those sintered at other heating rates.

## References

- [1] N. Miura, H. Kurosawa, M. Hasei, G. Lu, W. Yamazoe, Stabilized zirconia-based sensor using oxide electrode for detection of NOx in high-temperature combustion-exhausts, *Solid State Ionics* 86–88 (1996) 1069–1073.
- [2] M. Stoukides, C.G. Vayenas, The effect of electrochemical oxygen pumping on the rate and selectivity of ethylene oxidation on polycrystalline silver, *J. Catal.* 70 (1981) 137–146.
- [3] W. Huang, P. Shuk, M. Greenblatt, M. Croft, Q. Chen, M. Liuc, Structural and electrical characterization of a novel mixed conductor:  $\text{CeO}_2\text{--Sm}_2\text{O}_3\text{--ZrO}_2$  solid solution, *J. Electrochem. Soc.* 147 (2000) 4196–4202.
- [4] R.A. George, N.F. Bessette, Reducing the manufacturing cost of tubular solid oxide fuel cell technology, *J. Power Sources* 71 (1998) 131–137.
- [5] T. Kudo, H. Obayashi, Mixed electrical conduction in fluorite-type  $\text{Ce}_{1-x}\text{Gd}_x\text{O}_{2-x/2}$ , *J. Electrochem. Soc.* 123 (1976) 415–419.
- [6] P.D. Batle, C.R.A. Catlow, J.W. Heap, L.M. Moroney, Structural and dynamic studies of  $\delta\text{-Bi}_2\text{O}_3$  oxide ion conductors. I. The structure of  $(\text{Bi}_2\text{O}_3)_{1-x}(\text{Y}_2\text{O}_3)_x$  as a function of  $x$  and temperature, *J. Solid State Chem.* 63 (1986) 8–15.
- [7] T. Ishihara, T. Shibayama, S. Ishikawa, K. Hosoi, H. Nishiguchi, Y. Takita, Novel fast oxide ion conductor and application for the electrolyte of solid oxide fuel cell, *J. Eur. Ceram. Soc.* 24 (2004) 1329–1335.
- [8] H. Inaba, H. Tagawa, Ceria-base solid electrolytes, *Solid State Ionics* 83 (1996) 1–16.
- [9] S.W. Zha, C.R. Xia, G.G. Meng, Effect of Gd (Sm) doping on properties of ceria electrolyte for solid oxide fuel cells, *J. Power Sources* 115 (2003) 44–48.
- [10] T. Mori, Y. Wang, J. Drennan, G. Auchterlonie, J.G. Li, T. Ikegami, Influence of particle morphology on nanostructural feature and conducting property in Sm-doped  $\text{CeO}_2$  sintered body, *Solid State Ionics* 175 (2004) 641–649.
- [11] T. Mori, T. Ikegami, H. Yamamura, Application of a crystallographic index for improvement of the electrolytic properties of the  $\text{CeO}_2\text{--Sm}_2\text{O}_3$  system, *J. Electrochem. Soc.* 146 (1999) 4380–4385.
- [12] F.Y. Wang, S. Chen, S. Cheng,  $\text{Gd}^{3+}$  and  $\text{Sm}^{3+}$  co-doped ceria electrolytes for intermediate temperature solid oxide fuel cells, *Electrochem. Commun.* 6 (2004) 743–746.
- [13] X.L. Chen, W. Eysel, The stabilization of  $\beta\text{-Bi}_2\text{O}_3$  by  $\text{CeO}_2$ , *J. Solid State Chem.* 127 (1996) 128–130.
- [14] G.S. Li, L.P. Li, S.H. Feng, M.Q. Wang, L.Y. Zhang, X. Yao, An effective synthetic route for a novel electrolyte: nanocrystalline solid solutions of  $(\text{CeO}_2)_{1-x}(\text{BiO}_{1.5})_x$ , *Adv. Mater.* 11 (1999) 146–149.
- [15] Z.C. Li, H. Zhang, B. Bergman, X.D. Zou, Synthesis and characterization of IT-electrolyte of  $\text{La}_{0.85}\text{Sr}_{0.15}\text{Ga}_{0.85}\text{Mg}_{0.15}\text{O}_{3-\delta}$  by steric entrapment synthesis method, *J. Eur. Ceram. Soc.* 26 (2006) 2357–2364.
- [16] E.A. Benson, S.J. Lee, W.M. Kriven, Preparation of portland cement components by PVA solution polymerization, *J. Am. Ceram. Soc.* 82 (1999) 2049–2055.
- [17] WebElements periodic table, Web Site: <http://www.webelements.com> (2007).
- [18] K. Huang, R.S. Ticky, J.B. Goodenough, Superior perovskite oxide-ion conductor; strontium- and magnesium-doped  $\text{LaGaO}_3$ . I. Phase relationship and electrical properties, *J. Am. Ceram. Soc.* 81 (1998) 2565–2575.
- [19] B.C.H. Steel, Appraisal of  $\text{Ce}_{1-y}\text{Gd}_y\text{O}_{2-y/2}$  electrolyte for IT-SOFC operation at 500 °C, *Solid State Ionics* 129 (2000) 95–110.
- [20] S. Zha, C. Xia, G. Meng, Effect of Gd (Sm) doping on properties of ceria electrolyte for solid oxide fuel cells, *J. Power Sources* 115 (2003) 44–48.
- [21] H.L. Tuller, Ionic conduction in nanocrystalline materials, *Solid State Ionics* 131 (2000) 143–157.
- [22] A.V. Chadwick, in: J. Karger, F. Grinberg, P. Heitjans (Eds.), *Proceeding of the Diffusion Fundamentals Leipzig 2005*, Leipziger University, Leipzig, Germany, 2005, p. 204.
- [23] J. Maier, Ionic transport in nano-sized systems, *Solid State Ionics* 175 (2004) 7–12.